

Impacts of Groundwater Flow on Evolution of a Thermokarst Lake in the Permafrost Region on the Qinghai-Tibet Plateau

Wei Wang ^{1,2*}, Jinlong Li ^{1,2}, Xianmin Ke ^{1,2}, Kai Chen ^{1,2}, Zeyong Gao³, Fujun Niu³

1. School of Water and Environment, Chang'an University, Xi'an, 710054, Shaanxi, P.R.China

2. Key Laboratory of Subsurface Hydrology and Ecological Effect in Arid Region of the Ministry of Education, Chang'an University, Xi'an, 710054, Shaanxi, P.R.China

3. State Key Laboratory of Frozen Soil Engineering, Northwest Institute of Eco-Environmental and Resources, CAS, Lanzhou, 730000, P.R. China

*Corresponding author: Wei Wang (wangweichd@chd.edu.cn)

Abstract

Thermokarst lakes and permafrost degradation in the Qinghai-Tibet Plateau (QTP) resulting from global warming have been considerably affected the local hydrological and ecological process in recent decades. Simulation with coupled moisture-heat models that follows talik formation in the Beiluhe Basin (BLB) in the hinterland of permafrost regions on the QTP provides insight into the interaction between groundwater flow and freezing-thawing process. A total of 30 modified SUTRA schemes have been established to examine the effect of hydrodynamic forces, permeability and climate. The simulated results show that the hydrodynamic conditions impact the permafrost degradation surrounding the lake, thereby further affecting groundwater flow and late-stage freezing-thawing process. The thickness of the active layer varies with time and location under different permeability conditions, which significantly influences the occurrence of a breakthrough of the lake bottom. Warmer climate accelerates thawing and decreases the required time of formation of the breakthrough zone. Overall, these results indicate that explicit consideration of hydrologic process is critical to improve the understanding of environmental and ecological changes in cold regions.

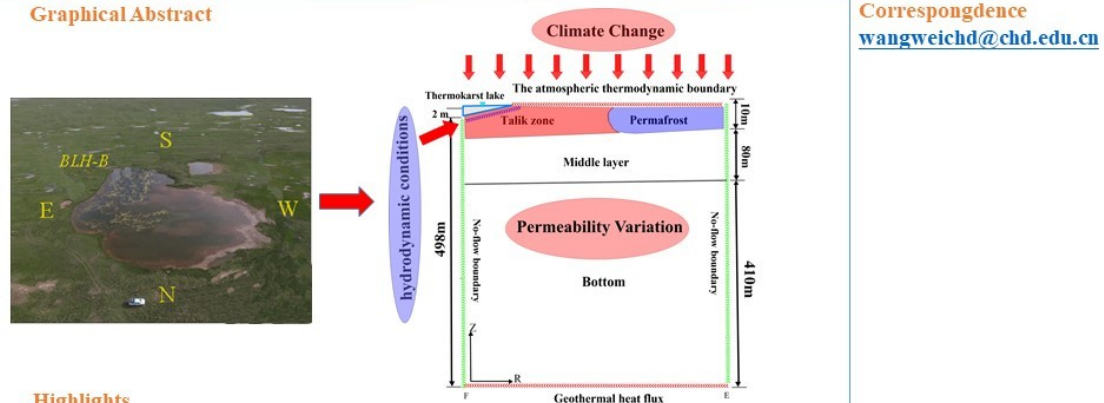
Keywords: Thermokarst lake; Groundwater flow; Permafrost; Numerical simulation; Qinghai-Tibet Plateau.

Graphical Abstract

Impacts of Groundwater Flow on Evolution of a Thermokarst Lake in the Permafrost Region on the Qinghai-Tibet Plateau

Wei Wang^{1,2*}, Jinlong Li^{1,2}, Xianmin Ke^{1,2}, Kai Chen^{1,2}, Zeyong Gao³, Fujun Niu³

Graphical Abstract



Correspondence
wangweichd@chd.edu.cn

Highlights

- Without groundwater flow, the thermokarst lakes have a negligible influence on the surrounding permafrost.
- Both the required time for forming talik zone and the thawing rate of permafrost increase along with increasing permeability.
- The breakthrough time could be determined at any given air temperature, permeability, and hydrodynamic conditions.

1.Introduction

Extent of ground surface settlement is affected by the thawing of ice-rich permafrost, and typically, thermokarst lakes form in closed depression areas (Niu et al., 2014). Thermokarst lakes, as a ubiquitous landscape feature, widely distribute in the ice-rich permafrost layer such as high plateau at low latitude (Niu et al., 2011; Li et al., 2020) or pan-Arctic lowlands such as Siberia, Alaska and Canada (Polishchuk et al., 2017), and is very sensitive to global climate changes that are physically possible to occur in the coming centuries (Zhang et al., 2001, 2005; Klein et al., 2007; Li et al., 2014). Several studies have evidenced that, the QTP, as the “Third Pole” and “Asian Water Tower”, has a substantial impact on global climate change and ensuring the safety of water resources in Asia (Li et al., 2014; Zou

et al., 2017; Gao et al., 2018; Dai et al., 2019). Numerous lakes and ponds in the QTP, approximately more than 1500 (Ling et al., 2012), are the consequence of permafrost degradation following post environmental disturbances (Lin et al., 2010; Jones et al., 2011). The accumulating number of thermokarst lakes induced by climate change, human activities, and permafrost degradation on the QTP (Luo et al., 2015; Niu et al., 2015) has been considered as an indicator and mainstay of permafrost variation. This suggests that a holonomic and significant mutual feed exists between thermokarst lakes and the global climate system (Karlsson et al., 2012). The mean annual temperature of these lakes has been significantly higher than the temperature of the surrounding land surface (Ling et al., 2003; Cheng et al., 2007), indicating that thermokarst lakes are the primary heat sources that accelerate permafrost degradation.

Furthermore, numerous studies have attempted to demonstrate that thermokarst lake is not only a significant factor responsible for altering landforms and ecosystem functions in high and cold regions (Lin et al., 2010; Levy et al., 2013; Séjourné et al., 2015), but changes both surface water and groundwater storage. Besides, substantial amounts of carbon released by the thawing permafrost exacerbate global warming (Wu et al., 2008; Ling et al., 2003). Therefore, it is essential to forecast and mitigate the impacts of permafrost degradation as well as its effects on global warming through a better understanding of the hydrological process, a thermokarst pond or lake and its surrounding permafrost.

A detailed characterization of hydrology in the Qinghai Tibet Plateau (QTP) or other cold regions is prerequisite to the main direction to explore the hydrological effect in permafrost systems. However, given that the thermokarst lake is distributed in the QTP, together with an average altitude of over 4000m above mean sea level (m.s.l.) under severe conditions (Zhou et al., 2000; Cheng and Wu, 2007; Ge et al., 2011), thereby making it difficult for the long-time direct monitoring and prediction of its

influence on permafrost degradation (Li et al., 2020; Li et al., 2014). It is important to note that an increasing number of studies have mainly used numerical models to examine the impacts of typical thermokarst lake or pond on both shallow and taliks (thawed regions beneath permafrost).

The majority of previous permafrost modeling studies have applied two directions of the coupled water-heat model. One consideration is the changes and exchange of water and heat within permafrost (Jansson et al., 2001; Jeffrey et al., 2007; Ji et al., 2012; Kelleners et al., 2013), while the other is considering the coupled processes in the ecosystems including atmosphere vegetation, and soil (Li et al., 2013; Ma et al., 2017). Understanding interactions between groundwater flow and permafrost dynamics is key to predicting the future change in water and energy balance of cold regions, particularly concerning the hydrologic effects (Hu et al., 2015; Lique et al., 2016; Walvoord & Kurylyk, 2016; Wrona et al., 2016). However, all the above-mentioned studies used heat conduction-based method to simulate the freezing-thawing process. Other processes caused by groundwater flow in discontinuous permafrost have not been taken into account (e.g. advective heat transport, heat migration) (Tristan and Michelle, 2013). Heat changes produced by heat conduction is generally regarded as the dominant force that accelerate underground ice to thaw and freeze, the effects of advective heat transport on the loss of ice beneath the lake have been neglected in most previous investigations. Moreover, despite extensive studies on the research of thermokarst lakes, the fundamental mechanisms responsible for the simulation of water movement and advective heat transport in the freezing-thawing process have not been fully elucidated. Therefore, while the temperature and climate changes are considered in previous work, the analysis of the impacts on permeability and hydrodynamic dynamics remains a knowledge gap that is yet to be filled in the permafrost science.

There are three important processes with regard to the formation of a thermokarst lake/pond, which include moisture migration, formation of ice lenses at freezing fringe, and water replenishment from the lake (Li et al., 2014). The studies of McKenzie et al (2007), and McKenzie and Voss (2012) have established a temperature affected model through simulating seasonal temperature fluctuations and ground-ice dynamics. Their investigations have revealed that the three processes are all affected by heat conduction and advective heat transport, which are generated by migration of groundwater flow. Thus, it is urgent and necessary to illuminate the hydrological process in permafrost area and reveal the influence mechanisms of permafrost distribution characteristics on groundwater system. To the best of our knowledge, only two studies, Ling (2012) and Li et al. (2014), have so far evaluated the thermal regime of permafrost underneath a thermokarst lake in QTP, while hydrological process based on groundwater flow in these regions is still blank.

To address these problems, this study investigates how groundwater flow impacts the evolution of thermokarst lakes. The aims of the work were to understand the interactions between groundwater flow and thermokarst lakes, and to quantify the water velocity and volume of thermokarst lakes under different conditions of three forms. The specific objectives of the study presented herein are to (1) clarify and evidence the significance of the role of hydrological cycle in the formation and evolution of thermokarst lakes, (2) and evaluate the influence of thermokarst lakes on the underneath and around permafrost, (3) ascertain the impacts of thermokarst lakes on regional groundwater. The variables explored in this study include the hydrodynamics (relationship between recharge and discharge of groundwater and lake water), permeability with regards to permafrost, and temperature changes with different climate. The outcomes of this study are expected to help provide insight into the interaction between thermokarst lakes and groundwater, as well as collectively serve as a reference for further

investigation on cold region science.

2.Methodology

To examine thermokarst lake dynamics and surrounding permafrost development in the QTP region, coupled groundwater flow and thermal transport is simulated through various energy and hydrodynamic conditions by permafrost and subjected to temperature variation with a long-term warming trend superimposed on the seasonal cycle. The results of the model are analyzed to quantify the influence of thermokarst lakes under different conditions on regional groundwater cycle caused by warming and thawing.

2.1 Model Description

The SUTRA code (Voss and Provost, 2002) has emerged as a powerful tool to simulate unsaturated flow, groundwater (saturated) flow, and heat or solute transport (Li et al., 2014; Zipper et al., 2018; Grenier et al., 2018; Wellman and Walvoord, 2013). The modified model described in McKenzie et al. (2007) can couple simulations of groundwater flow and heat transport in freezing and thawing process by describing variation in thermal conductivity and heat capacity for mixtures of water and ice. Meanwhile, changes in the effective permeability as impacted by ice content have also been included in McKenzie's codes (Wellman and Walvoord, 2012). Although numerous approaches have similar functions, this modified model is more practical and objective compared to other codes including freezing-thawing process (Zipper et al., 2018; Grenier et al., 2018).

The parameters describing general physical properties and ice functions are presented in Table 1. Notably, the heat transferred by both condensation and thawing of ice has substantial effects on heat transport, indicating that the sensible heat and latent heat during the ice water conversion should be fully considered. The effect of latent heat is far greater than that of heat capacities because of its dominant role in controlling the distribution of thermal regimes and ice (McKenzie et al., 2007). Thus,

latent heat released by ice water phase transition was described in modified code by considering the ice thermal conductivity and other parameters. The detailed simulation mechanism and governing equations have already been fully demonstrated in previous studies (McKenzie et al 2007, McKenzie and Voss 2013, Wellman et al 2013, Kurylyk et al 2016, Evans and Ge 2017, and Evans et al 2018). The model is run with three components to simulate freezing-thawing process, which included ice, liquid water, and thermal influence. Under the condition of saturation, the water-ice-heat coupling model of saturated soil can be described by mass conservation equation and energy conservation equation.

$$\left(S_w \rho_{Sop} + \varepsilon \rho \frac{\partial S_w}{\partial p} \right) \frac{\partial p}{\partial t} + \left(\varepsilon (\rho_i - \rho) \frac{\partial S_i}{\partial T} + \varepsilon S_w \frac{\partial \rho}{\partial T} \right) \frac{\partial T}{\partial t} - \nabla \cdot \left[\left(\frac{k k_r \rho}{\mu} \right) \cdot (\nabla p - \rho g) \right] = Q_p \quad (1)$$

Where Sop is the sum of the volume of water released in unit solid matrix due to the decrease of liquid pressure and pore volume, p is the pressure. t is the time, k is the permeability tensor, μ is the viscosity coefficient of liquid, and Q_p is the inflow volume of pore water. The equation.1 represents the mass balance of variable density pore water under the influence of temperature and pressure.

The equation.2 represents the heat balance of the formation under the conditions of heat conduction, heat convection and obtaining energy from other energy sources.

$$\left[\varepsilon \left(S_w \rho C_w + S_i \rho_i C_i \right) + (1 - \varepsilon) \rho_s C_s + \varepsilon \rho_i L_f \frac{\partial S_w}{\partial T} \right] \frac{\partial T}{\partial t} + \varepsilon S_w \rho C_w \underline{v} \cdot \underline{\nabla T} - \underline{\nabla} \cdot \left\{ \left[\varepsilon S_w \left(\lambda_w \underline{I} + \underline{D} \right) + \varepsilon S_i \lambda_i \underline{I} + (1 - \varepsilon) \lambda_s \underline{I} \right] \cdot \underline{\nabla T} \right\} = Q_p C_w (T^* - T) + \varepsilon S_w \rho \gamma_0^w + (1 - \varepsilon) \rho \gamma_0^s \quad (2)$$

Where \underline{I} is the identity tensor, \underline{D} is the dispersion tensor, T^* is the temperature of inflow liquid, γ_0^w

and γ_0^s represents the energy obtained by liquid and solid matrix, respectively.

Table 1.Parameters describing general physical properties and ice functions used in simulations.

Description	Value
Porosity(-)	0.25
Initial permeability(m2)	5×10^{-13} (490-500m), 1×10^{-13} (230-490m), 1×10^{-14} (0-230m)
Anisotropy(v/h)	1,1,1
Acceleration of gravity(m/s ²)	-9.81
Fluid specific heat(J·kg ⁻¹ ·°C ⁻¹)	4182
Density of fluid(kg·m ⁻³)	1000
Density of ice(kg·m ⁻³)	920
Latent heat of fusion(J·kg ⁻¹)	3.34×10^5
Fluid thermal conductivity(J/m·°C·h)	0.6
Fluid compressibility(kg/m·S ²)	0
Matrix compressibility(kg/m·S ²)	0
Solid grain specific heat(J·kg ⁻¹ ·°C ⁻¹)	1014
Solid grain conductivity(J/m·°C·h)	6566
Solid grain density(kg·m ⁻³)	1820
Maximum freezing temperature(°C)	0
Minimum freezing temperature(°C)	-1
Ice specific heat(J/Kg)	2108
Ice thermal conductivity(J/sm°C)	2.14
Air-land thermal conductivity(J/sm°C)	1
Freezing function	Non-Linear
Residual liquid water saturation	0.01
Relative permeability parameters	0.8

2.2 Simulation Description

2.2.1 Domain and Discretization

The basic scenario considered is the lake BLH-A (unofficial name, 34°49'30"N, 92°55'24"E), which has a total size of about 1.6 km² and an altitude of about 4600 m above sea level. It is surrounded by alluvial and pluvial originated highland (continuous permafrost) and is located in the Beiluhe basin (BLB), central QTP (Gao et al., 2018; Huang et al., 2019) (Fig.1). Lake BLA is an enclosed perennial lake, and the lake water provides abundant heat for the surrounding and underneath permafrost, thereby causing the lake bank to collapse.

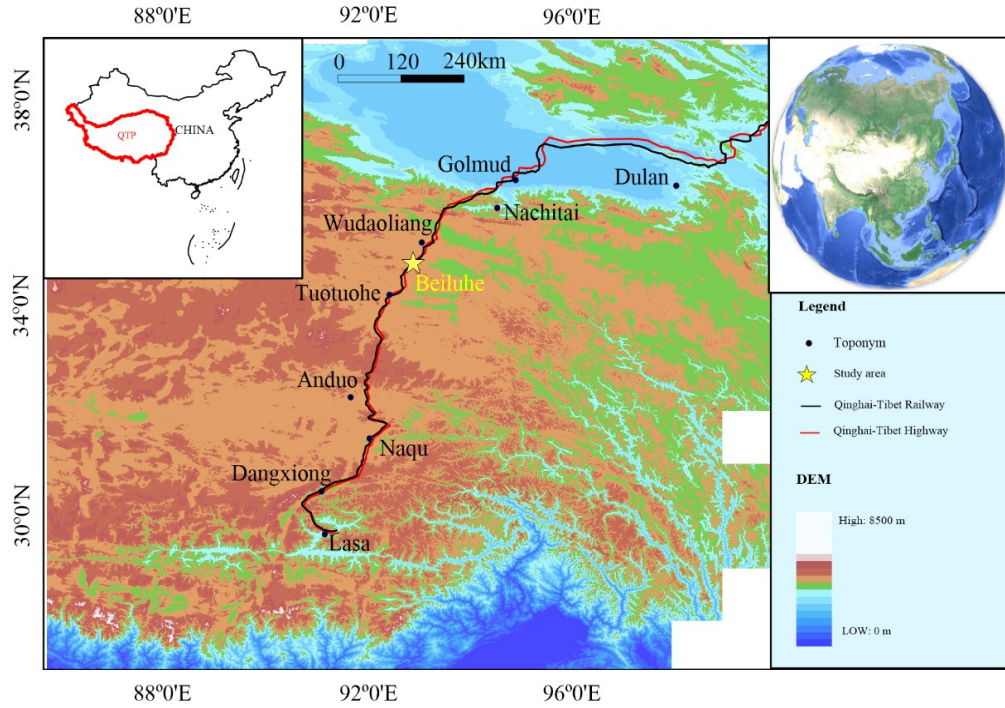
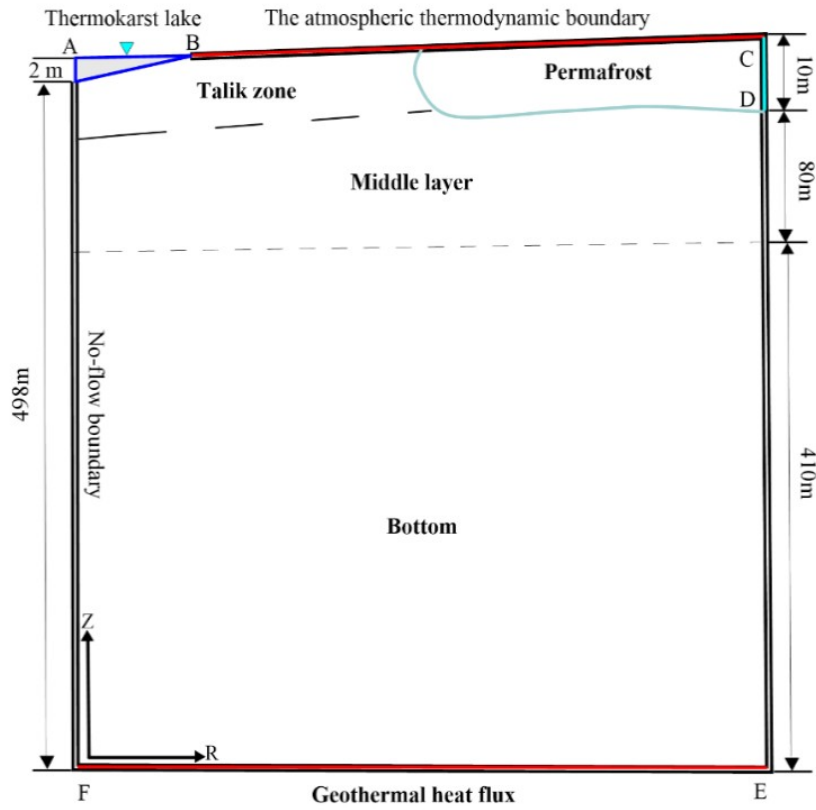
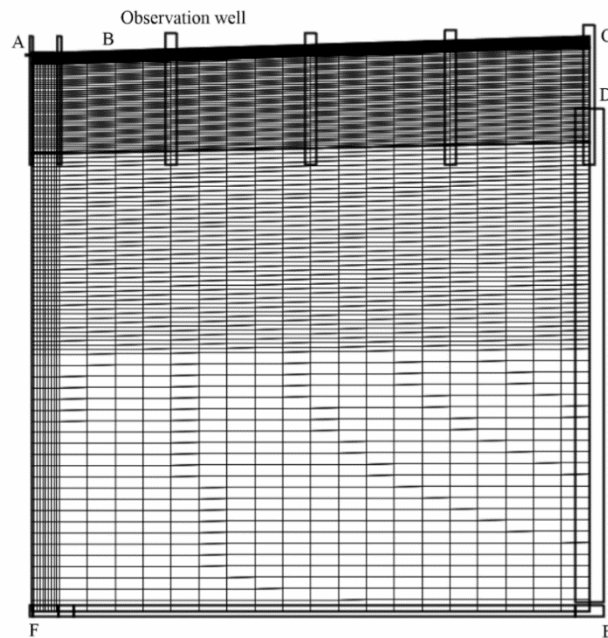


Figure 1. Geographical location of the study area in QTP, China.

A model with cylindrical coordinate system is built based on the above description of lake BLH-A. Its transverse direction was determined by the 1000m radial distance from the boundary of the outer drainage basin to the center of the lake (R , defined as 0m), and its longitudinal direction is determined by the elevation coordinate Z . The radial section of the model domain represents a generalized two dimensional 1000m slope (Fig.2). A 2m deep lake is formed on an 87m-thick permafrost layer, which it is about 0.016 degrees, according to the actual terrain slope of the study region (Niu et al., 2011).



a



b

Figure 2. (a) Cross section of two-dimensional (2D) cylindrical model (b).A discrete grid diagram of

model.

2.2.2 Boundary Conditions and Inputs

Thermal and hydraulic boundary conditions for each bottom side of the model were temporally constant. The atmospheric thermodynamic boundary (ABC) is specified as the top boundary to represent the authentic local pressure and temperature data, which is time-varying on a daily basis and is measured by the Beiluhe meteorological stations (Fig.3). Meanwhile, the variation of the lake bottom temperature is taken from the annual average temperature of the lake bottom measured in 2006 - 2016. The mesh resolution near the top is refined with a vertical discretization to capture spatial details of the seasonal freeze-thaw cycles within the aquifer, near the lake margins, and in deeper sections along the lake bottom (Fig.2.b). The bottom boundary is set as a no-fluid flow, with a large depth of 500m to minimize the influence of basal boundary conditions on shallow permafrost dynamics. The constant upward geothermal energy flux is set at 0.6W/m^2 , in accordance with the calculation results obtained from monitoring data at the lake BLH-A (Lin et al., 2013). The edge CD is set to a constant head boundary where the hydrodynamic conditions are considered (i.e., when the water head is higher than the lake bottom water level, the lake water is recharged by the underlying aquifer, while as the opposite conditions exist, the lake water is discharged into the aquifer). Thermal and hydraulic boundary conditions on the edge AF were set as no-flow based on the assumption of hydraulic symmetry around the stream at the center of the watershed.

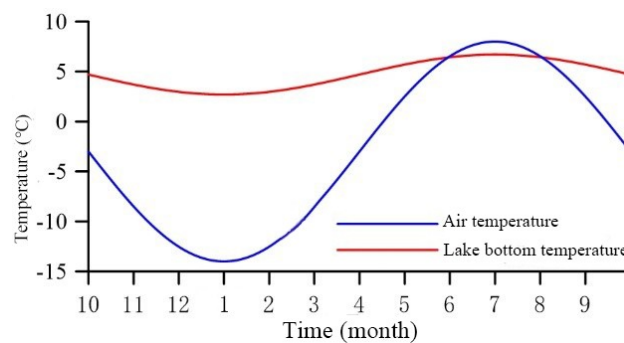


Figure 3. A sine function with a mean of -4°C and amplitude of 16°C with a $\pi/2$ phase shift was refined to described the air temperatures near the land surface, which causes subsurface temperatures at ~2m depth to approximate measured conditions typical of the region

Hydrogeological and geological characteristics are summarized in Fig.4, which representation follows the basic lithology of the simulation region. In order to ensure that the temperature of simulated groundwater is consistent with field observation, the mean annual lake bottom temperature observed in the field was utilized to correct the thickness of the upper aquifer section. The permeability value of the top layer is confined to the upper 490m of the aquifer through a series of iterative experiments. The permeability of the 10m-depth is set to 10-13 m2, which allows upward heat flux driven by heat conduction. The relatively high permeability values of geological layers are used to compare the maximum potential advection conditions with the hydrostatic pressure conditions, so as to develop a better understanding of different permeability conditions.

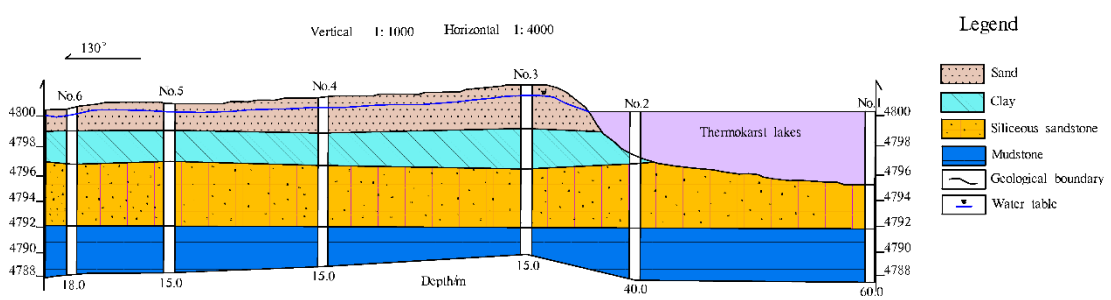


Figure 4. Hydrogeological cross section

2.2.3 Model Conditions

A total set of 30 scenarios was simulated to address variations in permeability, and hydrodynamic conditions (Table 2). These scenarios allow the whole freezing- thawing process of a typical thermokarst lake to be examined and the evolution of permafrost with continuous distribution and low topographic relief to be speculated.

Table 2. Scenarios simulated

Simulatio	Permeability	Temperature	Lake flow
-----------	--------------	-------------	-----------

n		
1		Initial
2		surface $-3\pm 11^{\circ}\text{C}$, lake $4.7\pm 2^{\circ}\text{C}$
3		Losing
4	upper $5\times 10\text{-}13\text{m}^2$, middle $1\times 10\text{-}$	Initial
5		surface $-3\pm 11^{\circ}\text{C}+0.03^{\circ}\text{C/yr}$, lake
6	13m^2 , bottom $1\times 10\text{-}14\text{m}^2$	$4.7\pm 2^{\circ}\text{C}+0.03^{\circ}\text{C/yr}$
7		Losing
8		Initial
9		surface $2\pm 11^{\circ}\text{C}$, lake $9.7\pm 2^{\circ}\text{C}$
10		Gaining
11		Losing
12		Initial
13	upper $5\times 10\text{-}12\text{m}^2$, middle $1\times 10\text{-}$	surface $-3\pm 11^{\circ}\text{C}+0.03^{\circ}\text{C/yr}$, lake
14		Gaining
15	12m^2 , bottom $1\times 10\text{-}13\text{m}^2$	$4.7\pm 2^{\circ}\text{C}+0.03^{\circ}\text{C/yr}$
16		Losing
17		Initial
18		surface $2\pm 11^{\circ}\text{C}$, lake $9.7\pm 2^{\circ}\text{C}$
19	Upper $5\times 10\text{-}14\text{m}^2$, middle	Gaining
20	$1\times 10\text{-}14\text{m}^2$, bottom $1\times 10\text{-}15\text{m}^2$	surface $-3\pm 11^{\circ}\text{C}$, lake $4.7\pm 2^{\circ}\text{C}$
21		Losing
22		Initial
23		Surface $-3\pm 11^{\circ}\text{C}+0.03^{\circ}\text{C/yr}$, lake
		Gaining

24		$4.7 \pm 2^\circ\text{C} + 0.03^\circ\text{C/yr}$	Losing
25			Initial
26		surface $2 \pm 11^\circ\text{C}$, lake $9.7 \pm 2^\circ\text{C}$	Gaining
27			Losing
28	upper $1 \times 10\text{-}40\text{m}^2$	surface $-3 \pm 11^\circ\text{C}$, lake $4.7 \pm 2^\circ\text{C}$	Initial
29		surface $-3 \pm 11^\circ\text{C} + 0.03^\circ\text{C/yr}$, lake	
	middle $1 \times 10\text{-}40\text{m}^2$	$4.7 \pm 2^\circ\text{C} + 0.03^\circ\text{C/yr}$	Gaining
30	bottom $1 \times 10\text{-}40\text{m}^2$	surface $2 \pm 11^\circ\text{C}$, lake $9.7 \pm 2^\circ\text{C}$	Losing

^a 0.03°C/yr : The surface temperature changed to $2 \pm 11^\circ\text{C}$ after 167 years, and the lake temperature changed to $9.7 \pm 2^\circ\text{C}$

^b Initial: H at the bottom of lake is equal to that at the same height of the vertical boundary of the model.

^c Gaining: H at the bottom of lake is 3 m smaller than that at the same height of the outer boundary of the model.

^d Losing: H at the bottom of lake is 3 m larger than that at the same height of the outer boundary of the model.

The flow direction of groundwater between the permafrost aquifer and the simulated lake can be

controlled by specifying the water head value at the outermost part of the model. The fluid pressure

along the vertical boundary of the permafrost aquifer model depends on the pressure of the static

aquifer. Head difference (ΔH) can be formed between the aquifer and the lake bottom by increasing or

decreasing the head value (H), thus causing a change in the flow direction of groundwater. The

hydrodynamic conditions are as follows: (1) H at the bottom of the thermokarst lake is consistent with

the water head at the same height of the external vertical boundary of the model; (2) H at the bottom of

the lake is 3m smaller than the outer boundary at same height. Meanwhile, the groundwater in the

upper part of the permafrost layer enters from the outer vertical aquifer boundary and acts as the linear

recharge source of the lake; (3) Moreover, ΔH , which is the difference between H at the lake

bottom and the outer boundary, is 3 m. As a result, the lake water enters into the aquifer and flows out

from the outer vertical aquifer boundary in the form of groundwater. Furthermore, the temperature of groundwater flowing into each position along the external pressure boundary can be determined according to the average surface temperature and the geothermal gradient of $35\text{ }^{\circ}\text{C}\cdot\text{km}^{-1}$.

Permeability is an important parameter which significantly influences the water movement and energy transmission. However, it has not been analyzed separately in previous studies. Permeability is determined for the solid matrix material, and reduced as a function of liquid pore water saturation using a relative permeability scaling coefficient (Zipper et al., 2018). Also, including groundwater flow increases the perceived importance of subsurface hydraulic properties, i.e. the soil permeability. Therefore, four permeability cases are presented herein (case 1 in Table 2), which can be subdivided into groundwater flow (cases 10 and 19) and no groundwater flow (case 28).

Rising temperature caused by global warming has an overall effect on the development of thermokarst lakes. In this regard, “normal”, “warmer”, and “high temperature” climate scenarios are utilized to test the hypothesis that groundwater flow will accelerate the freezing–thawing process as the temperature increases. The “warmer”, and “high temperature” scenarios use yearly changes modified from that of the normal climate by raising the temperature, as described in Table 2. The amplitude of seasonal fluctuations remains unchanged, while the adjustment of temperature is assumed to change as a mean increment. The selected rising temperature is based on 90-year projected RegCM3 annual average temperature increase for QTP (Niu et al., 2011).

3.Results

In comparison with other regions, energy exchange with water movement in cold regions have additional effects due to the freezing–thawing process in the subsurface and the existence and evolution of the permafrost structure in deeper regions (Wellman et al., 2013). Freezing–thawing process in the subsurface is induced by seasonal variations of surface temperature. The evolution of freezing–thawing

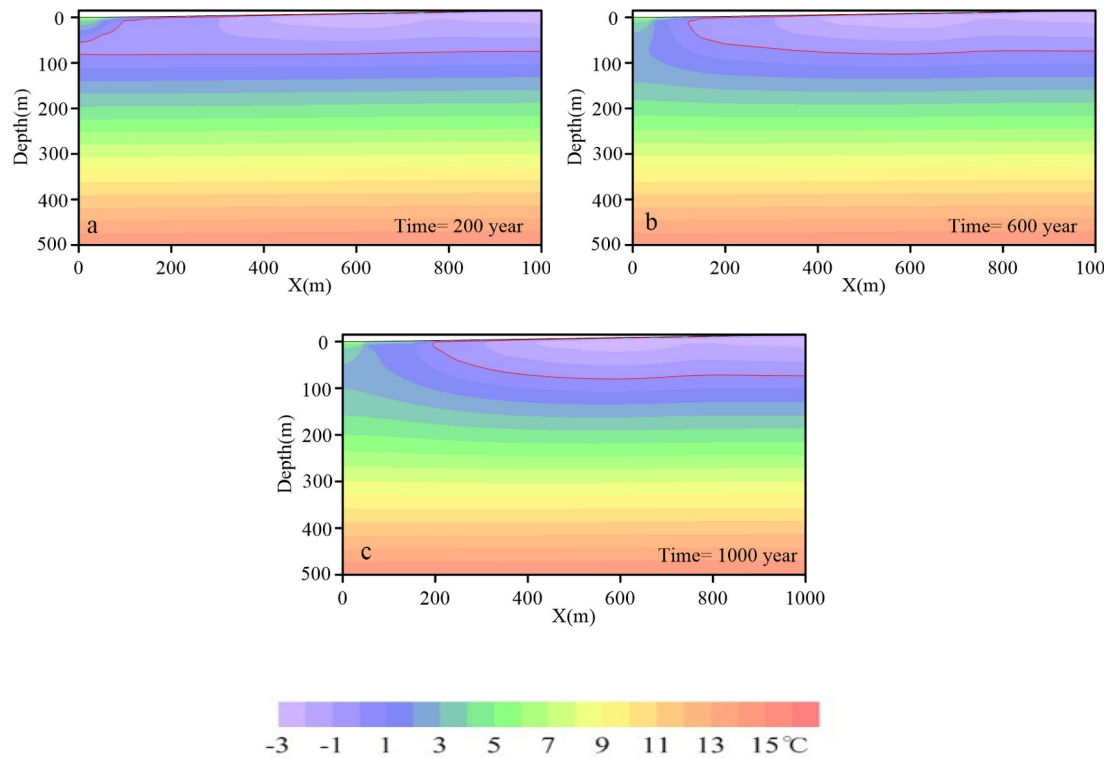
cycles near lake margins causes the hydraulic process to behave in a complex manner. There are three factors that have impacted hydrologic and thermal processes in cold regions: (1) hydrodynamic conditions (recharge and discharge conditions of groundwater), (2) formation permeability, and (3) climate. The simulation results are exploited to examine the effects of above three factors on the freezing–thawing process near the subsurface and the evolution of permafrost structure, as well as the hydraulic connection between the lake and groundwater.

3.1 Basic process of groundwater flow for a thermokarst lake system

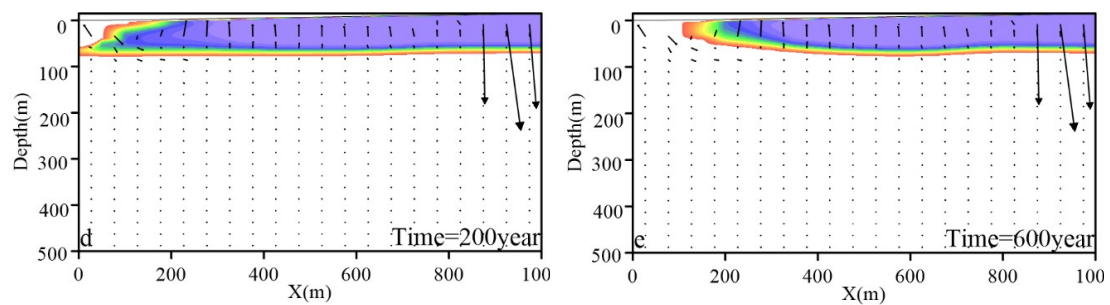
Detailed comparison of the simulation results under the current climate for the initial, losing, and gaining lake conditions with the actual formation permeability can comprehensively describe the relationship between freezing-thawing process and groundwater flow. Taking the initial lake as a sample, Fig.5 a-c illustrates the corresponding change in temperature with time elapsed since the lake formation for the initial, losing, and gaining lake conditions, respectively. Fig.5 d-g presents the temporal progression in both flow and ice volume.

Variations of groundwater flow and ice volume are shown in Fig. 5, suggesting that the variation trend of underground ice is basically consistent with the range of temperature below 0 °C. Soil with ice saturation greater than 0.9 is confined as high ice content frozen soil, because the soil cannot freeze completely due to the existence of residual water content in solid matrix. The area of high ice content frozen soil is less than that of the region with temperature below 0 °C, which indicates that most of the permafrost exists in the form of high ice content frozen soil. Furthermore, the range of frozen soil decreases with time, and the value of ice saturation gradually increases from the position where the temperature is less than 0 °C to the area with lower temperature. After breakthrough, the talik zone expands laterally outward from the lake center, further accelerating the melting of underground ice. The

length and the direction of the arrow indicate the velocity and direction of groundwater flow in Fig.5 b-g, respectively. The flow direction of groundwater near the surface is mainly a downward infiltration. The maximum velocity of groundwater is 2.66×10^{-6} m/s at the highest terrain. The underground water flow velocity in the deep layer is quite small with a minimum value of about 2.74×10^{-12} m/s.



a-c



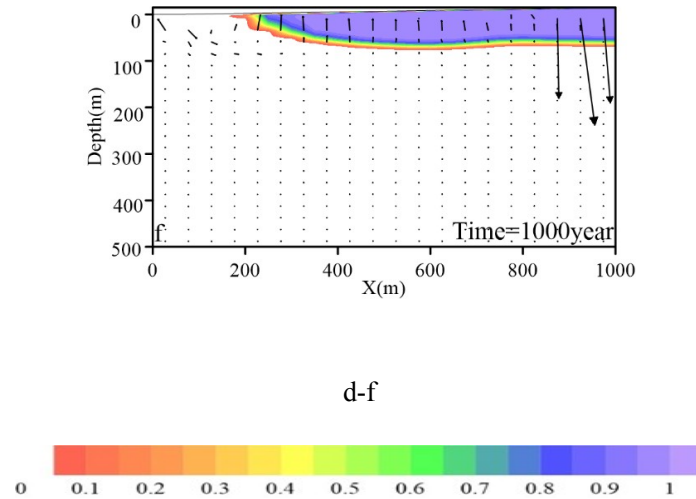


Figure 5. (a-c) Temperature profiles for 200, 600, and 1000 years. (d-f) volumetric ice content and velocity variation for 200, 600, and 1000 years (The length of the arrow represents the corresponding velocity and the direction of the arrow indicates the direction of groundwater movement). By changing the hydrodynamic conditions according to Table 2 and the operating scheme, it is concluded that the thermokarst lake breakthrough will occur in 219 years, 220 years and 216 years for the initial water lake, the gaining lake and the losing lake, respectively. Both the rate of total ice reduction and the groundwater flow under the lake will increase once an open freezing-thawing region is formed. The thaw rate is significantly increased due to the presence of thermal convection. However, the reduction of ice is ultimately controlled by heat conduction before freezing and thawing, because of the pore ice substantially impedes groundwater flow. After the ice structure of the lake edge becomes more balanced, the annual fluctuation of the ice volume in gaining lake and losing lake decreases with the passage of time.

Comparing the results of cases 1, 2, and 3, it can be concluded that the water flows into the ground from the bottom of the lake, and the temperature varies with seasons in a relatively large range. The discharge of lake water into aquifer is affected by the seasonal freezing and thawing of lakeside, and the flow between lake water and underlying aquifer fluctuates seasonally. For the gaining lake, the temperatures of incoming groundwater are less extreme prior to the formation of a talik zone, which

leads to a slightly slower reduction in ice volume at a rate that decreases over time. The freezing-thawing process around the lake will subside due to the inflow of groundwater, thus suppressing water exchange between the lake and the aquifer. The volume of permafrost with high ice saturation (ice saturation > 0.90) restricts groundwater movement, causing a relatively quick reduction in ice saturation, which is driven by heat conduction prior to talik formation. The distribution of permafrost is significantly affected by different permeability and hydrodynamic conditions with a normal atmospheric temperature.

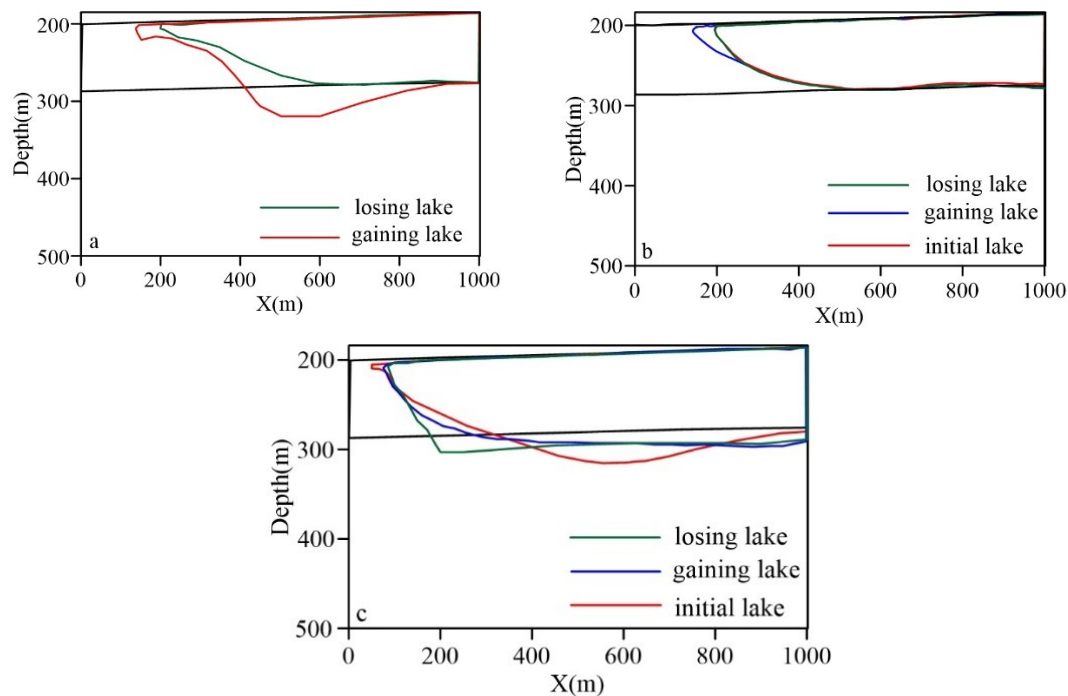


Figure 6. Distribution of permafrost under different permeability and hydrodynamic conditions. The range of color curve in above figure represents the domain of permafrost in different cases. (a) Higher permeability. (b) Actual permeability (c) Low permeability. Obviously, the high-temperature lake water transfers heat through thermal convection in the case of losing lake, causing the scope of thawing permafrost to increase. The 0°C isotherm near the lake is the steepest, because the downward flow of the lake water that flows into the aquifer promotes the thawing of the surrounding permafrost. In contrast to basic cases of models with different hydrodynamic conditions, the lower limit of permafrost fluctuates greatly with change in permeability (Fig.6).

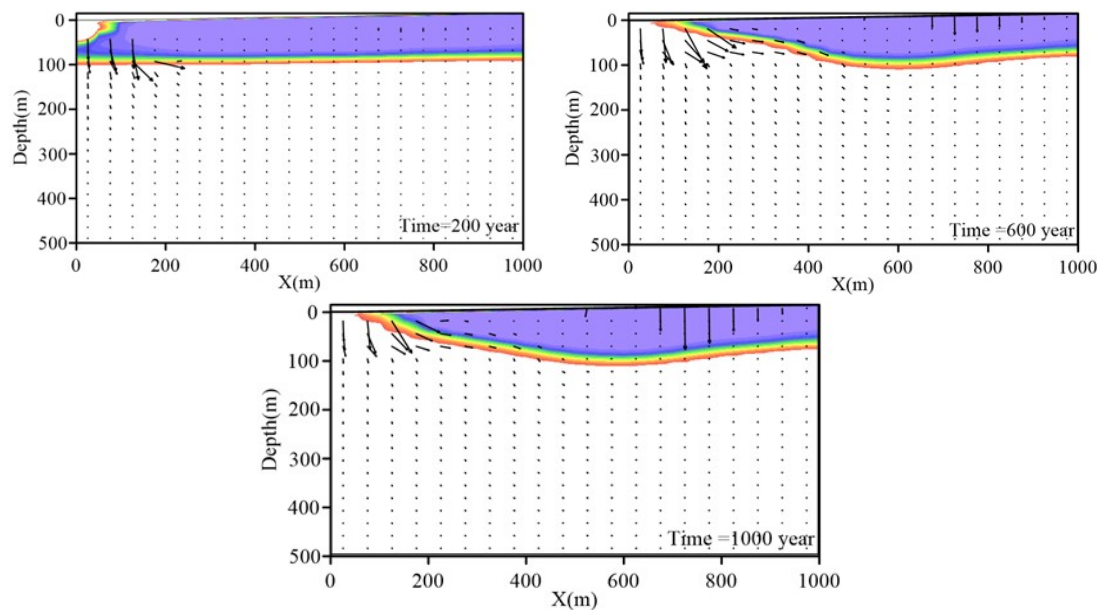
3.2 Development of the talik zone underlying the lake

Four cases of thermokarst lake evolution with different permeability are illustrated for the initial lake.

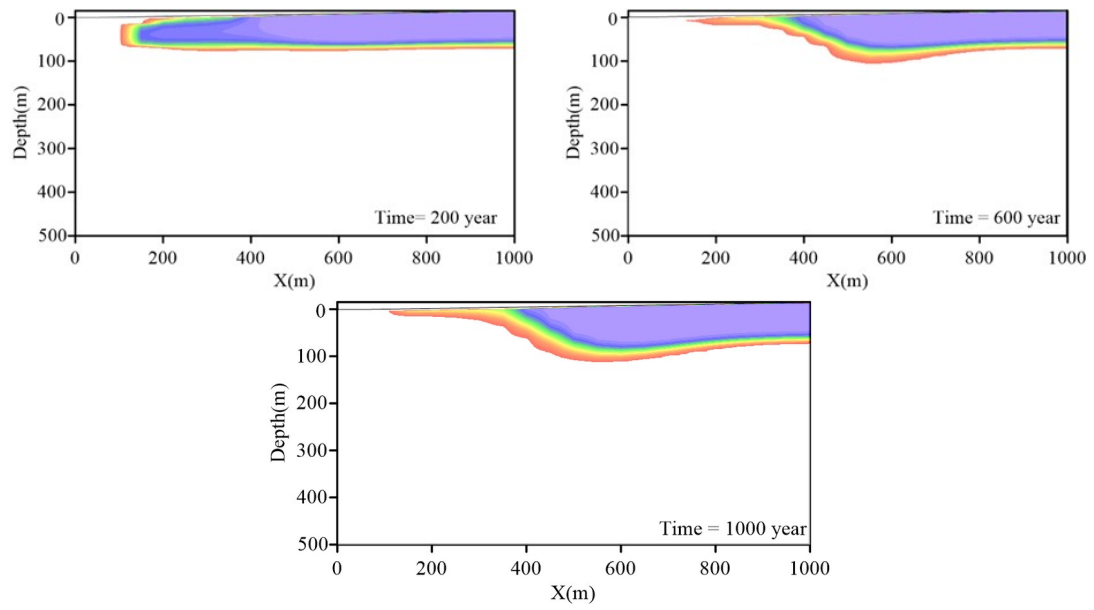
The results are examined at 200, 600, and 1,000-year elapsed times representing early to late phases in the talik development (Fig.7). The thawing process under all scenarios is controllable during the first 200 years.

The results showed that the breakthrough of these four cases would occur in 219 years for the initial scenario, 267 years for the larger permeability, 216 years for the smaller, and 826 years for minimal(which can be considered as a situation where there is no groundwater flow), respectively.

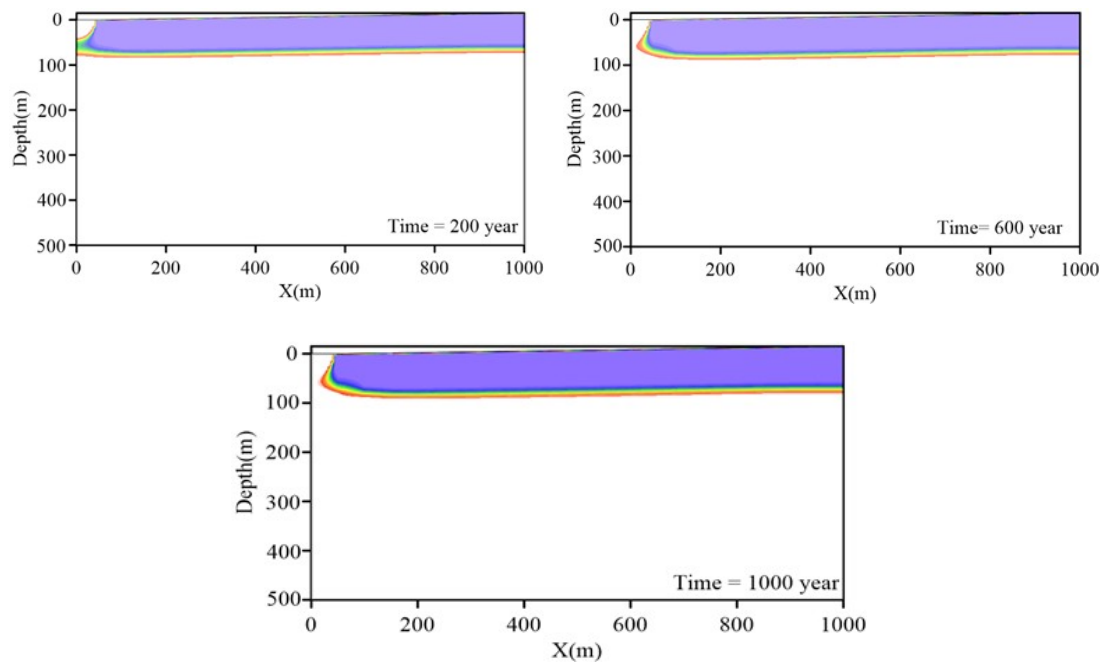
Obviously, the thickness of permafrost resulting from the initial state is thicker than that without groundwater flow. Regarding the case of groundwater participation, the permeability of permafrost is positively correlated with permafrost thickness. Topography has some influence on the formation of continuous permafrost, which leads to a parallel relationship between the lower limit of initial continuous permafrost and the surface. The distribution of permafrost in the stable state (1000 years) is presented in Fig.8.



(a)Case 10



(b)Case 19



(c)Case28



Figure 7. Results of thermokarst lake evolution with different permeability.

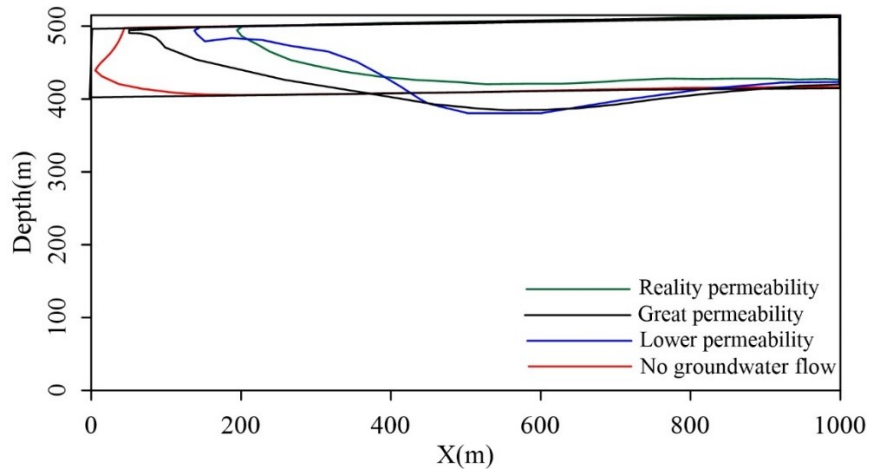


Figure 8. Distribution of permafrost under different permeability at the end of calculation.

At the stable state, the distribution of permafrost thickness in case 28 is the most uniform. The fluctuation of permafrost lower limit is the largest when the permeability is small. After thawing, the permafrost lower limit in the middle of the model decreases, while that at the boundary of the model rises. The affected range of permafrost around the lake is the largest in actual case scenario, whereas the influence on the permafrost near the lake is the least in the absence of groundwater flow.

Comparing the above four cases, it is seen that the required time for the formation of talik zone increases with increasing permeability. However, the required breakthrough time for permafrost layer in case 28 (the case without groundwater flow) is three to four times longer than that with groundwater flow. Furthermore, the thawing rate increases with increasing permeability, which is caused by the formation of thicker permafrost layer in the initial state when the formation permeability is maximum. Permeability has a strong influence on the temperature distribution in permafrost. Permafrost also shows a trend of being thick in the middle and thin on both sides, especially when permeability is quite small. Once the breakthrough occurs, the simulated lake BLH-A acts as a heat source and makes the soil degenerate through heat conduction. At the same time, thawing process of underground ice is accelerated through thermal convection of groundwater flow.

Due to the unique climate and environment of the QTP, the active layer is mostly formed during the period of high temperature from May to September, while the surface is frozen in other months. Therefore, the thickness of the active layer varies with time and location under different permeability conditions from May to September (Fig.9).

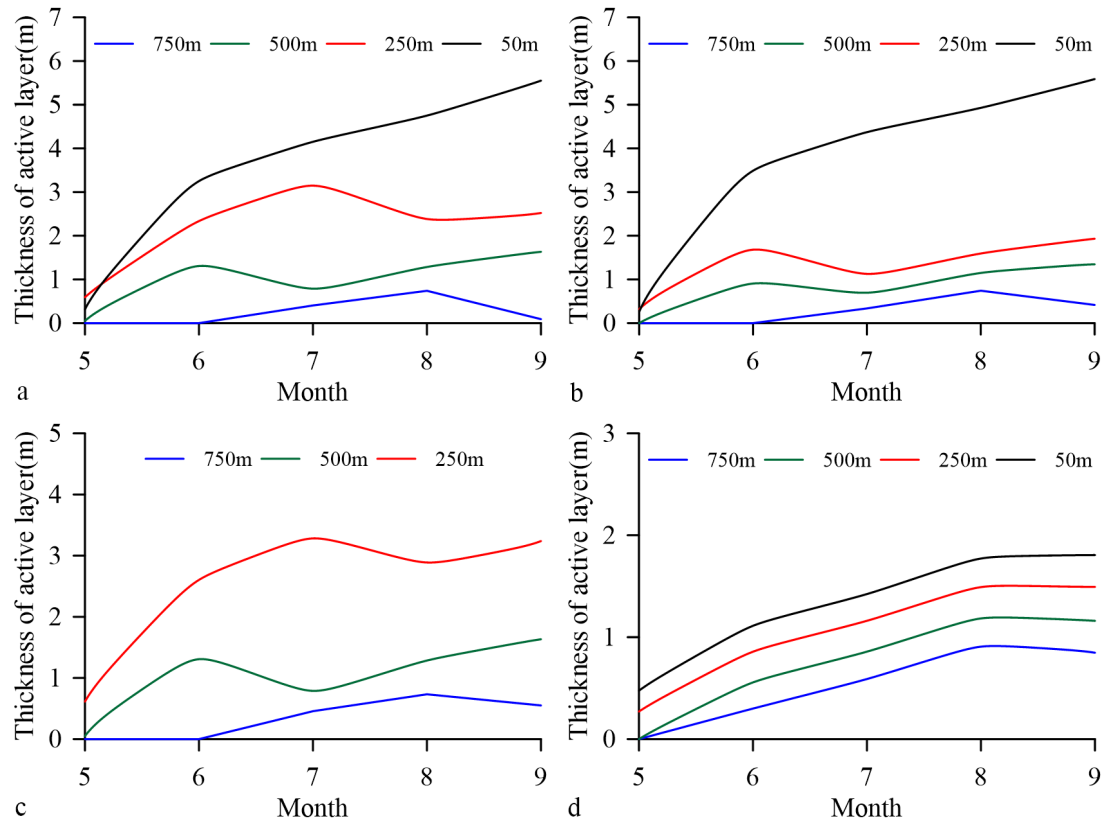


Figure 9. Monthly variation of active layer thickness at various positions on the surface. (a) Greater permeability (b) Actual permeability (c) Low permeability (d) No groundwater flow.

In the case of high permeability, the thickness of active layer reaches the maximum in September at 50m, 250m and 500m away from the lake. However, regarding the actual formation permeability, the thickness of active layer at each location fluctuates greatly with time, and the months with the maximum thickness of active layer are quite different. In the case of low permeability, the strata are completely melted through at 50m away from the center of the lake. The active layer thickness at different locations in case of no groundwater flow (case 18) continues to rise with a basically consistent ratio. Therefore, permeability plays a critical role in controlling thermal convection and heat

conduction between permafrost and groundwater flow. Permafrost near the outer boundary of the model is less affected by the lake, and can even be neglected. The flow direction of groundwater is vertically upward from the bottom of the model, and the heat of frozen soil is only provided by the temperature gradient of the stratum and the flow of groundwater.

3.3 Impacts of global warming on freezing-thawing process

Changes of temperature has an important effect on the freezing-thawing process and the development of the lake. Although extensive studies have indicated that global warming and human disturbance are the main factors responsible for the formation and development of thermokarst lakes, it is still unclear how they affect the correlation between groundwater flow and freezing-thawing process. To clarify this point, cases 1 (normal climate), 4(warmer climate), and 7(high temperature climate) are designed to explore the impact of temperature rise on groundwater flow and freezing-thawing process. Cases 4 and 7 simulate two states of global warming on the basis of the initial conditions, where the rising gradient is derived from results provided by China National Meteorological Administration.

The calculation results suggest that the permafrost underlying the lake will degenerate completely after more than 200 years. After the degradation, heat is transferred from the original freezing-thawing region to both top and bottom along with the direction of groundwater flow, causing the temperature at the corresponding point to increase. As a result, the temperature distribution shows a trend of first decreasing and then increasing from the subsurface to the bottom of the model. At the end of the calculation period of 1000 years, the lowest temperatures in the stratum of cases 4 and 7 are 2.84 °C (4) and 7.64 °C, respectively, and the corresponding surface temperatures are 9.02 and 10.61 °C. The highest surface temperature occurs on the surface of the lake due to the description of the lake boundary condition.

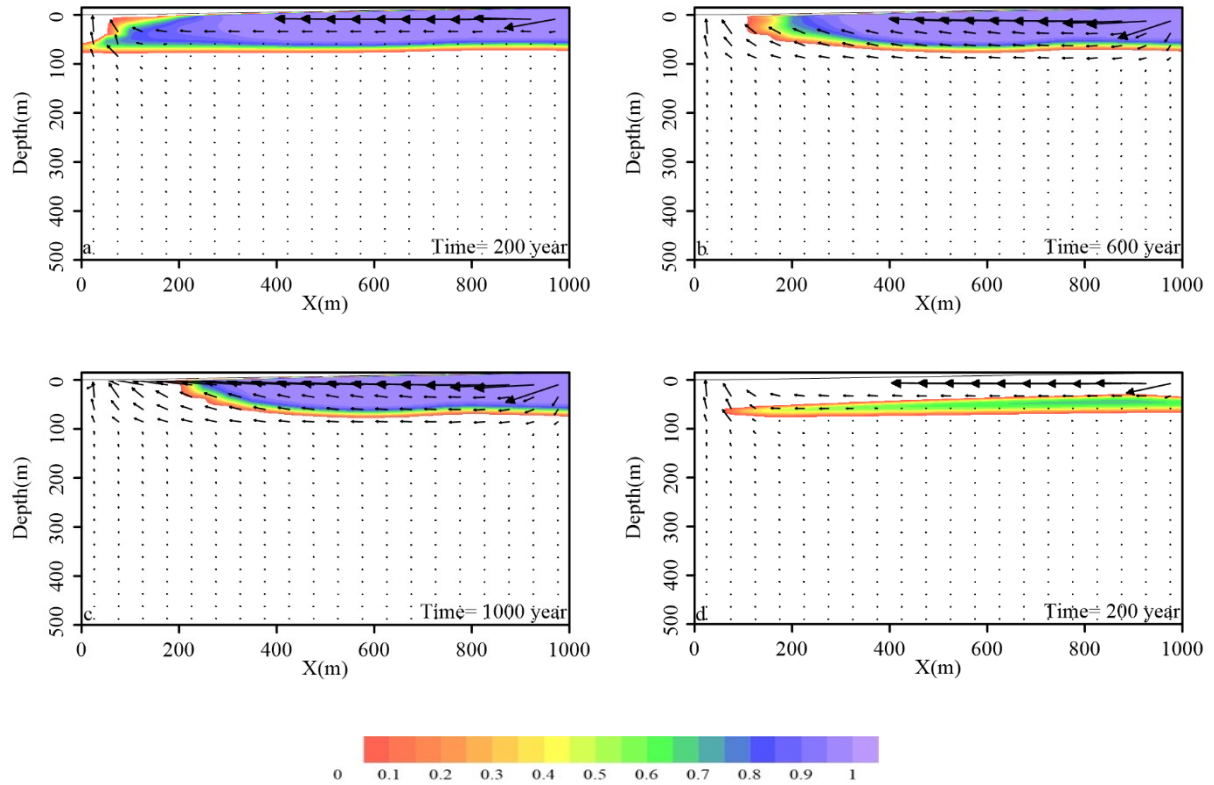


Figure 10. (a-c) Volumetric ice content and velocity variation of 200, 600, and 1000 year time periods for warmer climate. (d) Volumetric ice content and velocity variation of 200 year for high temperature climate.

The velocity range in the stratum is about 3.88×10^{-12} to 3.72×10^{-6} m / s in 200 years. Groundwater in the continuous permafrost layer flows toward the lake for all three cases, and groundwater at the bottom of the lake also converges to the lake. The formation of freeze-thaw zone is accelerated via heat conduction caused by groundwater flow. The maximum velocity is observed in the surface active layer, and the minimum velocity appears in the lower part of the model. The velocity at each position in the whole system increases significantly after the occurrence of breakthrough. However, there are no apparent variations in the direction and magnitude of velocity in a large time scale. As a result, groundwater continues to converge from all directions of the aquifer to the lake, causing shallow flow to become the dominant form of groundwater flow.

The distribution of permafrost under different conditions in 200 years is compared in order to explore

the influence of these conditions on the freezing-thawing process in the stratum. Results of permafrost degradation over 200 years are shown in Figure 10. Obviously, the lower limit of permafrost remains basically unchanged. On the contrary, the upper limit decreases markedly with rising temperature. In case of higher permeability, the degradation position of permafrost changes significantly along with different temperature conditions. The range of permafrost under the state of temperature rising is greater than that of high temperature, which is completely different from that in the case of low permeability. The whole permafrost is completely degraded under high temperature in the case of low permeability. In addition, permafrost is only distributed in a small range in the east domain under increasing temperature conditions.

4. Discussion

Permafrost-impacted regions are complex environments, in which their response to climate change depends on the multiple interactions among water, soil, topography, vegetation and snow (Niu et al., 2011; Wellman and Walvoord, 2013; Gao et al., 2018). A simplified coupled moisture-heat model is developed herein which includes freezing-thawing process, water movement, and lake development, modeled after lake BLH-A in the QTP. The breakthrough time, climate changes and hydrogeological control factors of the lake in this investigation are broadly applicable to the thermokarst lakes in the northern and central regions of the QTP with discontinuous permafrost. Limited information is available regarding the hydrogeological and ecological conditions in the QTP. Thus, the correlation between freezing-thawing process and groundwater flow presented in this study has a qualitative applicability to similar cold-region lake systems, while quantitative results will tend to be site specific.

The results show the influence of hydraulic conditions on the development of the thermokarst lake in cold region, which include hydrodynamic conditions and permeability. Based on the analysis of the

results, it is confirmed that the early thawing after the formation of the lake (200 years or less) is controlled by the heat conduction under the lake bed. Under different hydrodynamic conditions, groundwater circulation is dominated by shallow flow. At later time, the transfer of heat by groundwater flow is an important mechanism that accelerates permafrost thaw and expedites breakthrough of lake system.

Comparing cases 1 and 2, the 0 °C isotherm near the lake is the steepest while the lake water recharges groundwater, indicating that permafrost degradation is more severe. Furthermore, formation permeability has a far-reaching influence for permafrost degradation. The higher the permeability is, the more severe the permafrost degradation is. Namely, the hydraulic potential between lakes, permafrost aquifers and sub-permafrost aquifers enhances groundwater flow, thereby causing the heat advection in groundwater and expanding the speed and range of permafrost thaw for further gaining lakes and losing lakes. Changes in hydraulic conditions between lake and groundwater will accelerate the lake water / groundwater exchange, which mainly occurs between lake and permafrost aquifer. Also, the interaction between groundwater and surface-water will decrease, and time for talik zone formation becomes longer.

The modified code includes the effects of three actual conditions on the simulation results: (1) the influence of heat capacity and thermal conductivity of water and ice; (2) permeability of aquifer will reduce due to the formation of ice; (3) latent heat will be released when ice phase changes. Moreover, our guiding principle in model design is to establish a groundwater flow model in “the simplest way possible that captures the most important overall behavior” (Voss, 2011b,p. 1456). Thus, rather than building a highly parameterized site-specific calibrated model, we made several simplifying assumptions to isolate the aspects of the domain most relevant to our research questions on

hydrogeology of cold regions (Zipper et al., 2018; Soylu et al., 2017). Also, monitoring the lake hydrology in the QTP has proven to be difficult owing to logistical challenges and some uncertainties in the field while surveying (Li et al., 2020). Therefore, we simplified the lake BLH-A to a two-dimensional cross section similar to other previous studies on cold region simulation (Geet et al., 2011; Kurylyk et al., 2016; McKenzie et al., 2007; McKenzie & Voss, 2013; Wellman et al., 2013)

Despite the strong model performance when compared to field observations of freezing-thawing process in actual cold region, the present study has certain limitations. First, there are many other additional conditions that can be considered in the numerical simulation, such as the shape of the lake bottom, the size of the lake, terrain, and stratum, amongst others. However, the present study only focus on the subsurface. Therefore, it does not simulate ponding at the land surface, which may occur during snow melting or precipitation events if there is insufficient infiltration capacity. Additionally, only the influence of a single thermokarst lake was considered for regional groundwater. On this basis, the interaction between thermokarst lakes in different stages of development and surrounding groundwater, the interaction between multiple lakes or lake groups and the surrounding environment, and the influence of thermokarst lakes on climate change can be further investigated. This work promotes further research on the coupled water-heat process of permafrost around the thermokarst lakes/ponds in cold regions, towards providing a comprehensive understanding of the critical effects of groundwater flow in the freezing- thawing process.

5. Conclusion

As the key research object of ecological environment and hydrological effect in cold regions, the permafrost degradation represented by thermokarst lakes will inevitably lead to changes in the regional environment and have a certain impact on the regional groundwater system. The development of regional groundwater system can strengthen the hydraulic connection of permafrost regions through

heat conduction and thermal convection, which in turn can control the shape, location and structure of permafrost. The feedback mechanism between permafrost and groundwater finally forms a more complex system that has a further influence on the hydrological and ecological changes of the QTP.

The main conclusions from this study can be summarized as follows:

1) Thermokarst ponds or lakes have a great influence on the surrounding ground in the form of a heat source, especially the underlying permafrost. Permafrost surrounding the lake is mainly affected, especially as the hydrodynamic conditions change. Regardless of the hydrodynamic conditions, groundwater circulation is dominated by shallow flow.

2) Without groundwater flow, the distribution of permafrost thickness is the most uniform, indicating that thermokarst lakes have a negligible influence on the surrounding permafrost. Both the required time for forming talik zone and the thawing rate of permafrost increase along with increasing permeability. Under different permeability conditions, the active layer gradually thickens with decreasing distance from the active layer to the lake. The thermokarst lakes are mainly supplied by surface runoff and the upper permafrost water.

3) The thickness of permafrost and the time required to form breakthrough zone decrease with increasing atmospheric temperature. The thickest active layer at the same position and time occurs in the case of high temperature climate, while the thinnest active layer occurs at normal temperature.

4) According to the breakthrough time of the thermokarst pond for different cases, a cubic relationship of the breakthrough time with different conditions is obtained. According to this relationship, the time at which the talik penetrates the permafrost layer could be easily determined at any given air temperature, permeability, and hydrodynamic conditions.

Overall, although climate is generally believed to be the dominant environmental driving force in cold regions, groundwater flow is equally important in controlling the evolution of permafrost freezing and

thawing. Studies that evaluate changes in temperature, permeability, and hydrodynamic conditions and predict climate change and its impacts in cold regions should consider hydrological process and groundwater dynamics.

Acknowledgements

This research was mainly supported by Cold and Arid Regions Environmental and Engineering Research Institute, Chinese Academy of Sciences. This research was funded by National Science Foundation of China, Grant No. 41730640—Environmental and Hydrological Effects of the Thermokarst Lakes in the Permafrost Region of the QTP; and the Fundamental Research Funds for the Central Universities, CHD, Grant No. 300102290401. We also thank Penny Wang for her support on language.

Data Availability Statement

Some or all data, models, or code generated or used during the study are available from the corresponding author by request.

Reference

- Cheng, G., and T. Wu (2007), Response of permafrost to climate change and their environmental significance, Qinghai-Tibet Plateau, *J. Geophys. Res.*, 112, F02S03, doi:10.1029/2006JF000631.
- Dai, L., Guo, X., Zhang, F., Du, Y., Ke, X., Li, Y., Peng, C. (2019). Seasonal dynamics and controls of deep soil water infiltration in the seasonally-frozen region of the Qinghai-Tibet plateau. *Journal of Hydrology*, 571, 740-748. doi: 10.1016/j.jhydrol.2019.02.021
- Frampton, A., S. L. Painter, and G. Destouni (2013), Permafrost degradation and subsurface-flow changes caused by surface warming trends, *Hydrogeol. J.*, 21, 271–280.
- Gao, Z., Niu, F., Lin, Z., Luo, J., Yin, G., & Wang, Y. (2018). Evaluation of thermokarst lake water balance in the Qinghai-Tibet Plateau via isotope tracers. *Sci Total Environ*, 636, 1-11. doi: 10.1016/j.scitotenv.2018.04.103

Ge, S., J. McKenzie, C. Voss, and Q. Wu (2011), Exchange of groundwater and surface-water mediated by permafrost response to seasonal and long term air temperature variation, *Geophys. Res. Lett.*, 38, L14402, doi:10.1029/2011GL047911.

Grenier, C., Anbergen, H., Bense, V., Chanzy, Q., Coon, E., Collier, N., et al. (2018). Groundwater flow and heat transport for systems undergoing freeze-thaw: Inter comparison of numerical simulators for 2D test cases. *Advances in Water Resources*, 114, 196–218. <https://doi.org/10.1016/j.advwatres.2018.02.001>

Hu, F. S., Higuera, P. E., Duffy, P., Chipman, M. L., Rocha, A. V., Young, A. M., et al. (2015). Arctic tundra fires: Natural variability and responses to climate change. *Frontiers in Ecology and the Environment*, 13(7), 369–377. <https://doi.org/10.1890/150063>

Jansson P. E., Moon D. S. A coupled model of water, heat and mass transfer using object orientation to improve flexibility and functionality[J]. *Environmental Modelling & Software*, 2001, 16(1):37-46.

Jeffrey M. McKenzie, Clifford I. Voss, Donald I. Siegel. Groundwater flow with energy transport and water–ice phase change: Numerical simulations, benchmarks, and application to freezing in peat bogs[J]. 2007, 30(4):966-983.

Ji Z. Q., Xu X. Y., Zhao C. K. Study on Model of Heat and Moisture Transfer in Freezing Soil[J]. *Applied Mechanics and Materials*, 2012, 10(4)170-173.

Karlsson, J.M., Lyon, S.W., Destouni, G., 2012. Thermokarst lake, hydrological flow and water balance indicators of permafrost change in Western Siberia. *J. Hydrol.* 464–465, 459–466.

Kelleners T. J. Coupled Water Flow and Heat Transport in Seasonally Frozen Soils with Snow Accumulation[J]. *Vadose Zone Journal*, 2013, 12(4):108-112.

Klein, R. J. T., S. Huq, F. Denton, T. E. Dowing, R. G. Richels, J. B. Robinson, and F. L. Toth (2007), Inter-relationships between adaptation and mitigation, in *Climate Change 2007: Impacts, Adaptation and Vulnerability*, Contribution of Working Group II to the Fourth Assessment Report of the

Intergovernmental Panel on Climate Change, Cambridge Univ. Press, Cambridge, United Kingdom and New York, N. Y., U.S.A.

Li, J., Wang, W., Wang, D., Li, J., & Dong, J. (2020). Hydrochemical and Stable Isotope Characteristics of Lake Water and Groundwater in the Beiluhe Basin, Qinghai–Tibet Plateau. *Water*, 12(8), 2269. doi: 10.3390/w12082269

L.S., Kirpotin, S.N., Pokrovsky, O.S., 2017. Size distribution, surface coverage, water, carbon, and storage of thermokarst lakes in the permafrost zone of the Western Siberia Lowland. *WaterSA* 9:228. <https://doi.org/10.3390/w9030228>.

Li, S., H. Zhan, Y. Lai, Z. Sun, and W. Pei (2014), The coupled moisture-heat process of permafrost around a thermokarst pond in Qinghai-Tibet Plateau under global warming, *J. Geophys. Res. Earth Surf.*, 119, 836–853, doi:10.1002/2013JF002930.

Li, X.Y., Ma, Y.J., Huang, Y.M., 2016. Evaporation and surface energy budget over the largest high-altitude saline lake on the Qinghai-Tibet Plateau. *J. Geophys. Res.* 121, 10470–10485.

Li Yang. Derivation of coupled model of water and heat transfer in frozen soil based on porous media theory [J]. *Journal of Hebei University of Engineering (NATURAL SCIENCE EDITION)*, 2012 (3): 11-14

Lin, Z., F. Niu, Z. Xu, J. Xu, and P. Wang (2010), Thermal regime of a thermokarst lake and its influence on permafrost, Beiluhe basin, Qinghai-Tibet Plateau, *Permafrost Periglac. Processes*, 21, 315–324, doi:10.1002/ppp.692.

Lin Zhanju, Niu Fujun, Ge Jianjun, Wang Ping, Dong Yuanhong. Variation characteristics of typical thermal thaw lakes in the northern foot of Qinghai Tibet railway and its influence on the thermal condition of frozen soil [J]. *Glacial frozen soil*, 2010, 32 (2): 341-350

Ling, F., Q. Wu, T. Zhang, and F. Niu (2012), Modelling open-talik formation and permafrost lateral thaw under a thermokarst lake, Beiluhe Basin, Qinghai-Tibet Plateau, *Permafrost Periglac. Processes*, 23, 312–321, doi:10.1002/ppp.1754.

Lique, C., Holland, M. M., Dibike, Y. B., Lawrence, D. M., & Screen, J. A. (2016). Modeling the Arctic freshwater system and its integration in the global system: Lessons learned and future challenges. *Journal of Geophysical Research: Biogeosciences*, 121, 540–566.
<https://doi.org/10.1002/2015JG003120>

Ma Shuai, Sheng Yu, Cao Wei, et al. Numerical simulation of spatial distribution characteristics of permafrost in the source region of the Yellow River [J]. *Acta geographica Sinica*, 2017, 72 (9): 1621-1633

Niu, F.J., Cheng, G.D., Luo, J., Lin, Z.J., 2014. Advances in thermokarst lake research in permafrost regions. *Sci. Cold Arid Reg.* 6 (5), 0388–0397.

Niu, F., Lin, Z., Liu, H., Lu, J., 2011. Characteristics of thermokarst lakes and their influence on permafrost in Qinghai-Tibet Plateau. *Geomorphology* 132, 222–233.

Niu, F., Lin, Z., Lu, J., Luo, J., Wang, H., 2015. Assessment of terrain susceptibility to thermokarst lake development along the Qinghai–Tibet engineering corridor, China. *Environ. Earth Sci.* 73 (9), 5631–5642.

Painter, S.L., J.D. Moulton, and C.J. Wilson (2013), Modeling challenges for predicting hydrologic response to degrading permafrost, *Hydrogeol. J.*, 21, 221–224.

Polishchuk, Y.M., Bogdanov, A.V., Polishchuk, V.Y., Manasypov, R.M., Shirokova,

Jones, B. M., G. Grosse, C. D. Arp, M. C. Jones, K. M. Walter Anthony, and V. E.

Romanovsky (2011), Modern thermokarst lake dynamics in the continuous permafrost zone, northern Seward Peninsula, Alaska, *J. Geophys. Res.*, 116, G00M03, doi:10.1029/2011JG001666.

Séjourné, A., Costard, F., Fedorov, A., Gargani, J., Skorve, J., Massé, M., Mège, D., 2015. Evolution of the banks of thermokarst lakes in central Yakutia (Central Siberia) due to retrogressive thaw slump activity controlled by insolation. *Geomorphology* 241,31–40.

Voss CI, Provost AM (2002) SUTRA: a model for saturated-unsaturated variable-density ground-water flow with solute or energy transport. US Geol Surv Water Resour Invest Rep 02-4231

Walvoord, M. A., & Kurylyk, B. L. (2016). Hydrologic impacts of thawing permafrost-a review. *Vadose Zone Journal*,15(6). <https://doi.org/10.2136/vzj2016.01.0010>

Wrona, F. J., Johansson, M., Culp, J. M., Jenkins, A., Mård, J., Myers-Smith, I. H., et al. (2016). Transitions in Arctic ecosystems: Ecological implications of a changing hydrological regime. *Journal of Geophysical Research: Biogeosciences*, 121, 650–674. <https://doi.org/10.1002/2015JG003133>

Wu, Q., and T. Zhang (2008), Recent permafrost warming on the Qinghai-Tibetan Plateau, *J. Geophys. Res.*, 113, D13108, doi:10.1029/2007JD009539.

Wu, Q., Zhang, T., 2010. Changes in active layer thickness over the Qinghai-Tibetan Plateau from 1995 to 2007. *J. Geophys. Res.* 115, D09107. <https://doi.org/10.1029/2009JD012974>.

Zhang, T., R. G. Barry, D. Gilichinsky, S. S. Bykhovets, V. A. Sorokovikov, and J. Ye (2001), An amplified signal of climatic change in soil temperature during the last century at Irkutsk, Russia, *Clim. Change*, 49, 41–76.

Zhang, T., et al. (2005), Spatial and temporal variability in active layer thickness over the Russian Arctic drainage basin, *J. Geophys. Res.*, 110,D16101, doi:10.1029/2004JD005642.

Zhao, L., Ding, Y., Liu, G., Wang, S., Jin, H., 2010. Estimates of the reserves of ground ice in permafrost regions on the Tibet Plateau. *J. Glaciol. Geocryol.* 32 (1), 1–9.

Zhou, Y., D. Guo, G. Qiu, G. Cheng, and S. Li (2000), *Geocryology in China* [in Chinese], Science Press, pp. 1–34.

Zou, D., et al., 2017. A new map of permafrost distribution on the Tibetan Plateau. *Cryosphere* 11 (6), 2527.

Zipper, S. C., Lamontagne-Hallé, P., McKenzie, J. M., & Rocha, A. V. (2018). Groundwater controls on postfire permafrost thaw: Water and energy balance effects. *Journal of Geophysical Research: Earth Surface*, 123, 2677–2694. <https://doi.org/10.1029/2018JF004611>

Zipper, S. C., Soylu, M. E., Kucharik, C. J., & Loheide II, S. P. (2017). Quantifying indirect groundwater-mediated effects of urbanization on agroecosystem productivity using MODFLOW-AgroIBIS (MAGI), a complete critical zone model. *Ecological Modelling*, 359, 201–219. <https://doi.org/10.1016/j.ecolmodel.2017.06.002>